Title	Multiqubit maximally entangled states in the NMR model
Author(s)	Zhou, B; Tao, R; Shen, SQ
Citation	Physical Review A - Atomic, Molecular, And Optical Physics, 2004, v. 70 n. 2, p. 022311-1-022311-9
Issued Date	2004
URL	http://hdl.handle.net/10722/43461
Rights	Creative Commons: Attribution 3.0 Hong Kong License

Multiqubit maximally entangled states in the NMR model

Bin Zhou,[1,2] Ruibao Tao,[3,1] and Shun-Qing Shen[4]
[1]*Department of Physics, Fudan University, Shanghai 200433, China*
[2]*Department of Physics, Hubei University, Wuhan 430062, China*
[3]*Center for Theoretical Physics, Chinese Center of Advanced Science and Technology (World Laboratory), P. O. Box 8730, Beijing 100080, People's Republic of China*
[4]*Department of Physics, The University of Hong Kong, Hong Kong, China*
(Received 17 April 2004; published 19 August 2004)

A single-step operation is proposed to produce multiqubit maximally entangled states in the NMR model. In the scheme, all qubits are initially in the ground state, and one single pulse of a multifrequency coherent magnetic radiation is applied to manipulate simultaneously the "active states" that satisfy the resonant conditions while all other "inactive states" remain unchanged. An effective Hamiltonian is derived in a generalized rotating frame, which allows us to predict the time evolution of "active states" generated by the magnetic pulse. The magnetic pulse parameters, such as frequencies, phases, amplitudes, and duration time, are obtained analytically to implement a Bell state of two qubits and a Greenberger-Horne-Zeilinger state of three qubits. The scheme has been generalized to create an N-qubit entangled state. Two rules are found to calculate the magnetic pulse parameters numerically, which are required to realize entangled states for even and odd qubits, respectively. The rules are successfully checked in the cases of $4 \leqslant N \leqslant 10$. The relation of $\ln t_0$ and $\ln N$ is found to be linear, and the duration time t_0 is approximately proportional to $\sqrt{N}$.

DOI: 10.1103/PhysRevA.70.022311 PACS number(s): 03.67.Lx, 03.65.Ud, 76.90.+d

I. INTRODUCTION

Quantum computing, based on quantum superposition and entanglement, has enormous advantages over the classical Turing machine [1,2]. Up to now, many physical systems have been suggested as possible implementations of quantum computing and quantum information processing, such as ion traps [3], nuclear magnetic resonance (NMR) [4], cavity QED systems [5], Josephson junctions [6], quantum dots [7], and silicon-based nuclear spins [8]. Among the systems, NMR is particularly attractive because of the long decoherence time and is one of the most developed approaches. The Deutsch-Josza quantum algorithm [9–11], Grover's quantum search algorithm [12–14], the seven-qubit Shor quantum factoring algorithm [15], quantum error correction [16,17], quantum Fourier transform [18], the five-qubit order-finding algorithm [19], quantum teleportation [20], adiabatic quantum computation [21], decoherence-free quantum computation [22,23], and geometric quantum computation [24,25], etc., have been successfully implemented in NMR experiments.

Quantum entanglement is of fundamental interest in experimental tests of quantum mechanics [26,27] and also plays a key role in quantum computing and quantum information processing [28,29]. It becomes significant in techniques to generate entangled states, especially multiple-particle entangled states. Implementing multiple-particle entangled states is an extremely challenging task. In recent years, the NMR technique has made some important experimental progress in this respect. Chuang *et al.* succeeded in creating Bell states using an effective pure state as an input in their two-spin NMR system [30]. The idea of using NMR to demonstrate Greenberger-Horne-Zeilinger (GHZ) correlations was proposed by Lloyd [31], and an effective GHZ state was first generated by Laflamme *et al.*, whose experiment appears to be the first time that a quantum network was used to systematically entangle more than two qubits [32]. Experimental realization of GHZ correlations was also reported by using NMR in Ref. [33]. Knill *et al.* generated a seven-qubit "cat state" which consists of an equal superposition of two states: one with all spins up and the other with all spins down [34]. Recently, an entanglement transfer on a four-qubit liquid-state NMR quantum information processor was implemented [35].

Lloyd described a method to perform an arbitrary quantum circuit by a sequence of electromagnetic pulses with well-defined frequency and amplitude in a weakly coupled quantum system [1,36]. The implementation of multiqubit entangled states mentioned above in NMR experiments involves a special sequence of magnetic pulses. For instance, in Laflamme *et al.*'s experiment a simple circuit to create a GHZ state consists of a rotation by $\pi/2$ around the y axis followed by two controlled-NOT gates on other qubits, and adapting this circuit to their system results in the pulse sequence shown in Fig. 2(b) of Ref. [32]. For simplicity, we consider the ground state $|00\cdots0\rangle$ as the initial state in an N-qubit system. The entangled state $(|00\cdots0\rangle + |11\cdots1\rangle)/\sqrt{2}$ ("cat state") can be generated by using a Hadamard gate followed by $(N-1)$ Λ_n (NOT) gates (or $N-1$ controlled-NOT gates [37]). The Λ_n (NOT) gate can be described by a unitary matrix [38]

$$\Lambda_n(\mathrm{NOT}) = \begin{pmatrix} I_{2^{n+1}-2} & 0 \\ 0 & \sigma_x \end{pmatrix}, \tag{1}$$

where $I_{2^{n+1}-2}$ is the $(2^{n+1}-2)\times(2^{n+1}-2)$ identity matrix, and σ_x is the Pauli matrix. Λ_1(NOT) is the so-called controlled-NOT gate, and Λ_2(NOT) the Toffoli gate. Figure 1 shows quantum circuits to create a Bell state and a GHZ state from

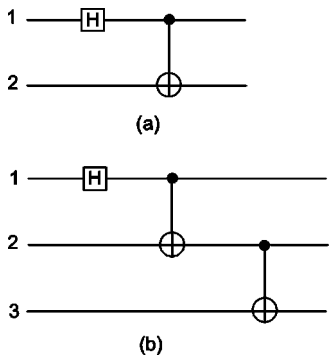

FIG. 1. Quantum circuits to create maximally entangled states from the initial ground states. (a) Two-qubit system; (b) three-qubit system.

the initial ground states $|00\rangle$ and $|000\rangle$ for two-qubit and three-qubit systems, respectively. The quantum circuits for larger N-qubit systems can be derived by analogy. Obviously, the number of required operations increases linearly with the number of qubits. Moreover, most implementation of the controlled-NOT gate in a liquid-state NMR also involves a special sequence of resonance electromagnetic pulses [30,38]. Note that Du *et al.* realized Λ_2(NOT) and Λ_3(NOT) gates in three- and four-qubit NMR systems experimentally using a single transition pulse with well-defined frequency and amplitude [38]. In addition, Berman *et al.* also investigated numerically a single-electromagnetic-pulse implementation of a quantum controlled-NOT gate in NMR model [39,40].

In this paper, a single-step operation is proposed to produce multiqubit maximally entangled states in the NMR model with well-resolved coupling. Unlike the previous schemes using a special sequence of magnetic pulses, to our best knowledge our proposal is the first to use only one pulse in the NMR model. It is assumed that the initial state is the ground state $|00\cdots0\rangle$. The key of our proposal is to design one single pulse of a multifrequency coherent magnetic radiation with well-defined frequencies, phases, amplitudes, and duration time. The multifrequency magnetic pulse is applied to manipulate simultaneously the "active states" which satisfy the resonant conditions while all other "inactive states" remain unchanged. The idea of a multifrequency magnetic pulse was presented theoretically in quantum information processing with large-spin systems [41–43]. In Sec. II, we describe how to generate the maximally entangled Bell state $(|00\rangle+e^{i\phi}|11\rangle)/\sqrt{2}$ of two qubits by means of a single-step operation in the NMR model. In Sec. III, we further discuss implementation of the maximally entangled GHZ state $(|000\rangle+e^{i\phi}|111\rangle)/\sqrt{2}$ of three qubits. In Sec. IV, we extend this to generate the entangled cat states of N qubits. Two rules are presented to calculate numerically the magnetic pulse parameters that are required to realize entangled states of any even and odd qubits, respectively, and the rules are checked for the cases of $4\leqslant N\leqslant 10$. In particular, it is interesting to observe that duration time t_0 of the magnetic pulse is approximately proportional to $\sqrt{N}$. Section V is devoted to the conclusions.

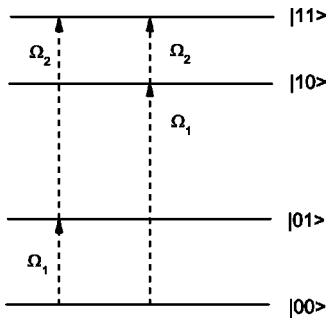

FIG. 2. The sketch of the energy levels of the Hamiltonian $H_{2\ \mathrm{qubit}}$ and two multiphoton transition schemes to generate $|\Psi_{\mathrm{Bell}}\rangle$. The dashed lines present the single-spin transitions. $\Omega_{1(2)}$ is the resonant frequency of the transverse magnetic pulse.

II. THE BELL STATE OF TWO QUBITS

To present a systematic description on a single-step operation proposal, we start with the maximally entangled Bell state. It is assumed that two qubits are initially in the ground state $|00\rangle$. In the following we will show how to design a single pulse of a multifrequency coherent magnetic radiation that can generate the maximally entangled Bell state $|\Psi_{\mathrm{Bell}}\rangle=(|00\rangle+e^{i\phi}|11\rangle)/\sqrt{2}$ in the NMR model. Consider a two-spin NMR model in which one spin interacts with the other spin through the Ising interaction. The Hamiltonian is

$$H_{2\ \mathrm{qubit}}=-\frac{1}{2}\left(\omega_1\sigma_1^z+\omega_2\sigma_2^z+\frac{J}{2}\sigma_1^z\sigma_2^z\right), \tag{2}$$

where $\omega_{1(2)}$ is the Larmor frequency for spin 1 (2) in a very strong static magnetic field, J is the interaction constant between nuclei, and $\sigma_{1(2)}^z$ is the $\hat{z}$ component of the Pauli matrix of spin 1 (2) (the units are such that $\hbar=1$). We assume that $\omega_1>\omega_2$ and $J\ll\omega_1-\omega_2$. For example, we choose that $\omega_1/(2\pi)=500$ MHz, $\omega_2/(2\pi)=100$ MHz, and $J/(2\pi)=10$ MHz. The complete set of eigenstates of Hamiltonian $H_{2\ \mathrm{qubit}}\{|00\rangle,|01\rangle,|10\rangle,|11\rangle\}$ is defined as a complete and orthogonal set of basis states, and the corresponding eigenenergies are $\varepsilon_1=-(\omega_1+\omega_2+J/2)/2$, $\varepsilon_2=-(\omega_1-\omega_2-J/2)/2$, $\varepsilon_3=-(-\omega_1+\omega_2-J/2)/2$, and $\varepsilon_4=-(-\omega_1-\omega_2+J/2)/2$, respectively. The sketch of the energy levels of Hamiltonian $H_{2\ \mathrm{qubit}}$ is shown in Fig. 2.

Now the problem becomes to find one magnetic pulse that leads to a unitary time evolution of the spins and produces the expected maximally entangled Bell state $|\Psi_{\mathrm{Bell}}\rangle$. To achieve this aim, we add an applied rectangular transversal magnetic pulse with two frequencies Ω_1 and Ω_2 to the two-qubit system. Figure 2 shows two possible schemes, and as an illustration, we choose the right scheme. Thus, the total Hamiltonian reads

$$H_{\mathrm{total}}^{(2)}=H_{2\ \mathrm{qubit}}+H_{\mathrm{pulse}}^{(2)}, \tag{3}$$

where

$$H_{\text{pulse}}^{(2)} = -\frac{1}{4}\sum_{i,k=1}^{2} h_{ik}(e^{i(\Omega_k t+\Phi_k)}\sigma_i^{+} + e^{-i(\Omega_k t+\Phi_k)}\sigma_i^{-}). \quad (4)$$

Here, $\sigma^{\pm}=\sigma^x \pm i\sigma^y$, $h_{1k}=g_1\mu H_k(t)$, and $h_{2k}=g_2\mu H_k(t)$. g_1 and g_2 are the g factors of two nuclear spins and different, and μ is the nuclear magneton. $H_k(t)$ $(k=1,2)$ is a pulse: $H_k(t)=H_k$ for $0<t<t_0$, and 0 otherwise. The phases Φ_k and duration time t_0 of the alternating magnetic field will be studied below in detail. In the current scheme, the frequency of the external magnetic field Ω_1 is resonant with the frequency of the transition $|00\rangle \leftrightarrow |10\rangle$, and the frequency Ω_2 with the transition $|10\rangle \leftrightarrow |11\rangle$, i.e., $\Omega_1=\omega_1+J/2$ and $\Omega_2=\omega_2-J/2$. Then, starting from the ground state $|00\rangle$, a pulse with two frequencies Ω_1 and Ω_2 leads only to a coherent evolution of three basis states $|00\rangle$, $|10\rangle$, and $|11\rangle$. The basis states, which satisfy the resonant conditions and can be manipulated simultaneously by a multifrequency magnetic pulse, are the so-called "active states." The remaining state $|01\rangle$ is the so-called "inactive state," which does not satisfy the resonant conditions and remains unchanged. In this case, the Hamiltonian (3) is truncated approximately as

$$H^{(2)} = \varepsilon_1|00\rangle\langle 00| + \varepsilon_3|10\rangle\langle 10| + \varepsilon_4|11\rangle\langle 11| + \left(\frac{h_1}{2}e^{i(\Omega_1 t+\Phi_1)}|00\rangle\langle 10| + \frac{h_2}{2}e^{i(\Omega_2 t+\Phi_2)}|10\rangle\langle 11| + \text{H.c.}\right), \quad (5)$$

where $h_1=h_{11}$ and $h_2=h_{22}$. The time-dependent Schrödinger equation reads $i\partial|\Psi(t)\rangle/\partial t=H^{(2)}|\Psi(t)\rangle$, where the evolution of the quantum state $|\Psi(t)\rangle$ from the initial state $|\Psi(0)\rangle(=|00\rangle)$ under the Hamiltonian $H^{(2)}$ [Eq. (5)] can be expressed as

$$|\Psi(t)\rangle = c_1(t)|00\rangle + c_2(t)|10\rangle + c_3(t)|11\rangle. \quad (6)$$

Now we are in the position to extract an effective Hamiltonian, which governs the expected unitary evolution, and leads to an analytic solution to this problem. We apply the generalized rotating frame [42,44] to eliminate the time dependence of $H^{(2)}$ by means of a unitary transformation

$$U(t) = e^{-i(\Omega_1 t+\Phi_1)}|00\rangle\langle 00| + |10\rangle\langle 10| + e^{i(\Omega_2 t+\Phi_2)}|11\rangle\langle 11|, \quad (7)$$

such that an equivalent Hamiltonian $H_{\text{rot}}^{(2)}$ is obtained [45],

$$H_{\text{rot}}^{(2)} \equiv U(t)H^{(2)}U^{+}(t) - iU(t)\,\partial U^{+}(t)/\partial t = \begin{bmatrix} 0 & \frac{h_1}{2} & 0 \\ \frac{h_1}{2} & 0 & \frac{h_2}{2} \\ 0 & \frac{h_2}{2} & 0 \end{bmatrix}. \quad (8)$$

The eigenstates and eigenvalues of $H_{\text{rot}}^{(2)}$ are

$$|\varphi_1\rangle = \frac{h_1}{\sqrt{2}\Delta}|00\rangle + \frac{1}{\sqrt{2}}|10\rangle + \frac{h_2}{\sqrt{2}\Delta}|11\rangle, \quad (9a)$$

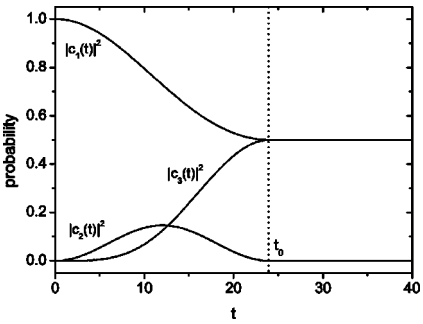

FIG. 3. Time evolution of the probabilities $|c_i(t)|^2$ subjected to the magnetic pulse for the two-qubit NMR model. The dotted line indicates the end of the rectangular pulse. The values of the parameters are $\omega_1/(2\pi)=500$ MHz, $\omega_2/(2\pi)=100$ MHz, $J/(2\pi)=10$ MHz, $\Omega_1/(2\pi)=505$ MHz, $\Omega_2/(2\pi)=95$ MHz, $h_1/(2\pi)=0.1$ MHz. $h_2/h_1=1+\sqrt{2}$. The duration time $t_0=24\ (2\pi\ \text{MHz})^{-1}$.

$$|\varphi_2\rangle = \frac{h_2}{\Delta}|00\rangle - \frac{h_1}{\Delta}|11\rangle, \quad (9b)$$

$$|\varphi_3\rangle = \frac{h_1}{\sqrt{2}\Delta}|00\rangle - \frac{1}{\sqrt{2}}|10\rangle + \frac{h_2}{\sqrt{2}\Delta}|11\rangle, \quad (9c)$$

and

$$E_1 = \frac{1}{2}\Delta,\ E_2 = 0, \quad E_3 = -\frac{1}{2}\Delta, \quad (10)$$

where $\Delta=\sqrt{h_1^2+h_2^2}$. The propagator of the form $U^{+}(t)e^{-iH_{\text{rot}}^{(2)}t}$ determines $c_i(t)$ $(i=1,2,3)$. Thus, with the initial condition $c_1(0)=1$ and $c_2(0)=c_3(0)=0$, we have the time evolution of the system as follows:

$$c_1(t) = \frac{1}{\Delta^2}[h_2^2 + h_1^2\cos(\Delta t/2)]e^{i(\Omega_1 t+\Phi_1)}, \quad (11a)$$

$$c_2(t) = \frac{h_1}{\Delta}\sin(\Delta t/2)e^{-i\pi/2}, \quad (11b)$$

$$c_3(t) = \frac{h_1 h_2}{\Delta^2}[1-\cos(\Delta t/2)]e^{-i(\Omega_2 t+\Phi_2)+i\pi}. \quad (11c)$$

The expected maximally entangled Bell state $|\Psi_{\text{Bell}}\rangle$ requires that the basis states $|00\rangle$ and $|11\rangle$ are simultaneously populated with equal amplitudes, i.e., $|c_1(t_0)|^2=|c_3(t_0)|^2=1/2$ and $|c_2(t_0)|^2=0$. From Eqs. (11a)–(11c), one can deduce the solution of the duration time of the pulse $t=t_0=2\pi/\Delta$, and two solutions for h_2/h_1: $h_2/h_1=1+\sqrt{2}$ or $h_2/h_1=-1+\sqrt{2}$. For the first solution, $h_2/h_1=1+\sqrt{2}$, the phase ϕ in the Bell state $|\Psi_{\text{Bell}}\rangle=(|00\rangle+e^{i\phi}|11\rangle)/\sqrt{2}$ is determined by $\phi=\pi-(\Omega_1+\Omega_2)t_0-(\Phi_1+\Phi_2)$, and $\phi=-(\Omega_1+\Omega_2)t_0-(\Phi_1+\Phi_2)$ for the second solution $h_2/h_1=-1+\sqrt{2}$.

According to the two different solutions of the field amplitudes, the generation processes of the Bell state as a function of time are shown in Fig. 3 (for $h_2/h_1=1+\sqrt{2}$) and Fig. 4 (for $h_2/h_1=-1+\sqrt{2}$), respectively, for the parameters $\omega_1/(2\pi)=500$ MHz, $\omega_2/(2\pi)=100$ MHz, $J/(2\pi)=10$ MHz,

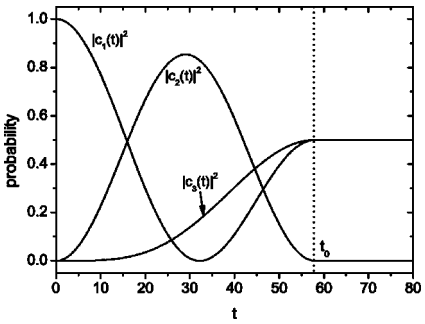

FIG. 4. Time evolution of the probabilities $|c_i(t)|^2$ subjected to the magnetic pulse for the two-qubit NMR model. The dotted line indicates the end of the rectangular pulse. The values of the parameters are $\omega_1/(2\pi)=500$ MHz, $\omega_2/(2\pi)=100$ MHz, $J/(2\pi)=10$ MHz, $\Omega_1/(2\pi)=505$ MHz, $\Omega_2/(2\pi)=95$ MHz, $h_1/(2\pi)=0.1$ MHz. $h_2/h_1=-1+\sqrt{2}$. The duration time $t_0=58\ (2\pi\ \mathrm{MHz})^{-1}$.

$\Omega_1/(2\pi)=505$ MHz, $\Omega_2/(2\pi)=95$ MHz, and $h_1/(2\pi)=0.1$ MHz. Obviously, the generation time (duration time t_0) of the Bell state is shortened by stronger pulses. In short, we have presented a single-step operation to produce a maximally entangled Bell state of two qubits in the NMR model. The Bell state with an arbitrary phase can be generated by using a two-frequency pulse with well-defined frequencies, phases, amplitudes, and duration time. Note that we use J coupling on the order of 10 MHz, which is higher than a typical J-coupling value in NMR quantum computing experiments. In order to implement the scheme on a two-qubit system with J coupling on the order of 100 Hz, according to the requirement of the conservation condition of energy $\delta t_0 \gg 1$ (here, δ is the detuning of the pulse frequency with respect to the resonant condition $\delta \sim J$), it is estimated that the duration time t_0 may be on the order of 0.1 s. This duration time is reasonable for typical decoherence times in NMR quantum computing experiments.

III. THE GHZ STATE OF THREE QUBITS

In this section we study how to generate the maximally entangled GHZ state $|\Psi_{\mathrm{GHZ}}\rangle=(|000\rangle+e^{i\phi}|111\rangle)/\sqrt{2}$ in a three-qubit NMR model by means of a single multifrequency pulse. The initial state is still assumed to be the ground state $|000\rangle$. In this case, we must use a rectangular circularly polarized transverse magnetic field pulse with three frequencies Ω_1, Ω_2, and Ω_3. Then the evolution of the system with the three-qubit NMR model under the action of this magnetic pulse is described by the following Hamiltonian:

$$H^{(3)}_{\mathrm{total}} = H_{3\ \mathrm{qubit}} + H^{(3)}_{\mathrm{pulse}}, \tag{12}$$

where

$$H_{3\ \mathrm{qubit}} = -\frac{1}{2}\sum_{i=1}^{3}\left(\omega_i\sigma_i^z + \sum_{j=2(j>i)}^{3}\frac{J_{ij}}{2}\sigma_i^z\sigma_j^z\right), \tag{13}$$

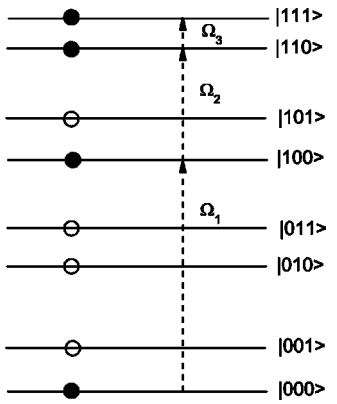

FIG. 5. The sketch of the energy levels of the Hamiltonian $H_{3\ \mathrm{qubit}}$ and a multiphoton transition scheme to generate $|\Psi_{\mathrm{GHZ}}\rangle$. The dashed lines present the single-spin transitions. The black and empty circles indicate the active states and inactive states in this scheme, respectively. $\Omega_{1(2,3)}$ is the resonant frequency of the transverse magnetic pulse.

$$H^{(3)}_{\mathrm{pulse}} = -\frac{1}{4}\sum_{i,k=1}^{3} h_{ik}(e^{i(\Omega_k t+\Phi_k)}\sigma_i^+ + e^{-i(\Omega_k t+\Phi_k)}\sigma_i^-), \tag{14}$$

with $\omega_1>\omega_2>\omega_3$ and $J_{ij}\ll\omega_i-\omega_j$. For example, we take $\omega_1/(2\pi)=500$ MHz, $\omega_2/(2\pi)=250$ MHz, $\omega_3/(2\pi)=100$ MHz, $J_{12}/(2\pi)=20$ MHz, $J_{23}/(2\pi)=10$ MHz, and $J_{13}/(2\pi)=2$ MHz. The basis states $\{|000\rangle,|001\rangle,|010\rangle,|011\rangle,|100\rangle,|101\rangle,|110\rangle,|111\rangle\}$ make up the Hilbert space of the Hamiltonian $H_{3\ \mathrm{qubit}}$. A sketch of the energy levels of the Hamiltonian $H_{3\ \mathrm{qubit}}$ is shown in Fig. 5. Figure 5 also shows a multiphonon transition scheme to produce the expected maximally entangled GHZ state $|\Psi_{\mathrm{GHZ}}\rangle$. In this scheme, the frequency of the external magnetic field Ω_1 corresponds to the frequency of the transition $|000\rangle\leftrightarrow|100\rangle$, Ω_2 to $|100\rangle\leftrightarrow|110\rangle$, and Ω_3 to $|110\rangle\leftrightarrow|111\rangle$, i.e., $\Omega_1=\omega_1+J_{12}/2+J_{13}/2$, $\Omega_2=\omega_2-J_{12}/2+J_{23}/2$, and $\Omega_3=\omega_3-J_{23}/2-J_{13}/2$. According to the conservation laws of energy and angular momentum, starting from an initial state $|000\rangle$, a pulse with three frequencies Ω_1, Ω_2, and Ω_3 induces a coherent evolution of only four basis states $|000\rangle$, $|100\rangle$, $|110\rangle$, and $|111\rangle$, and four other basis states remain unchanged. This is a necessary condition for our scheme. In Fig. 5, the active states and inactive states are indicated by the black and open circles, respectively.

Now the problem is reduced to one in a four-level subspace consisting of four active states. For convenience, we denote $|000\rangle\rightarrow|0\rangle$, $|100\rangle\rightarrow|1\rangle$, $|110\rangle\rightarrow|2\rangle$, and $|111\rangle\rightarrow|3\rangle$. Then the Hamiltonian (12) is truncated as follows:

$$H^{(3)} = \sum_{n=0}^{3}\varepsilon_n|n\rangle\langle n| + \sum_{n=1}^{3}\left(\frac{h_n}{2}e^{i(\Omega_n t+\Phi_n)}|n-1\rangle\langle n| + \mathrm{H.c.}\right), \tag{15}$$

where $h_1=h_{11}$, $h_2=h_{22}$, and $h_3=h_{33}$. ε_n is the eigenvalue of the Hamiltonian $H_{3\ \mathrm{qubit}}$ corresponding to the active state (eigenstate). The evolution of the quantum state $|\Psi(t)\rangle$ under the Hamiltonian $H^{(3)}$ (15) can be expressed as

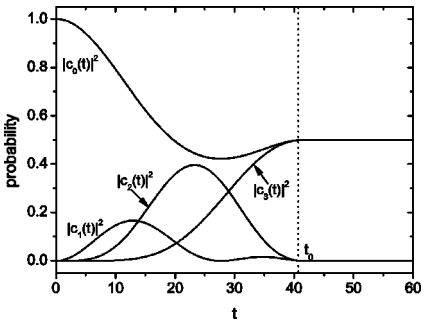

FIG. 6. Time evolution of the probabilities $|c_i(t)|^2$ subjected to the magnetic pulse for the three-qubit NMR model. The dotted line indicates the end of the rectangular pulse. For the first set of parameters $h_1/(2\pi)=0.1$ MHz, $h_3=h_1$, $h_2/h_1=6/\sqrt{7}$. The duration time $t_0=41.56\ (2\pi\ \mathrm{MHz})^{-1}$

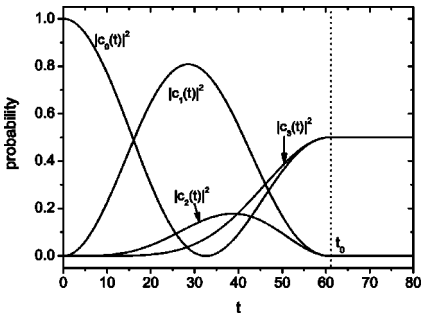

FIG. 7. Time evolution of the probabilities $|c_i(t)|^2$ subjected to the magnetic pulse for the three-qubit NMR model. The dotted line indicates the end of the rectangular pulse. For the second set parameters $h_1/(2\pi)=0.1$ MHz, $h_3=h_1$, $h_2/h_1=2/\sqrt{15}$. The duration time $t_0=60.84\ (2\pi\ \mathrm{MHz})^{-1}$

$$|\Psi(t)\rangle = c_0(t)|0\rangle + c_1(t)|1\rangle + c_2(t)|2\rangle + c_3(t)|3\rangle. \quad (16)$$

Likewise, the generalized rotating frame [42,44] is again applied to eliminate the time dependence of $H^{(3)}$ by means of a unitary transformation

$$U(t) = |0\rangle\langle 0| + e^{i(\Omega_1 t+\Phi_1)}|1\rangle\langle 1| + e^{i[(\Omega_1+\Omega_2)t+(\Phi_1+\Phi_2)]}|2\rangle\langle 2| + e^{i[(\Omega_1+\Omega_2+\Omega_3)t+(\Phi_1+\Phi_2+\Phi_3)]}|3\rangle\langle 3|, \quad (17)$$

such that an equivalent Hamiltonian $H_{\mathrm{rot}}^{(3)}$ is obtained,

$$H_{\mathrm{rot}}^{(3)} = \begin{bmatrix} 0 & \frac{h_1}{2} & 0 & 0 \\ \frac{h_1}{2} & 0 & \frac{h_2}{2} & 0 \\ 0 & \frac{h_2}{2} & 0 & \frac{h_3}{2} \\ 0 & 0 & \frac{h_3}{2} & 0 \end{bmatrix}. \quad (18)$$

The eigenstates $|\varphi_k\rangle$ and eigenvalues E_k $(k=1,2,3,4)$ of $H_{\mathrm{rot}}^{(3)}$ can also be found explicitly (see the Appendix). A propagator of the form $U^{+}(t)e^{-iH_{\mathrm{rot}}^{(3)}t}$ determines the phases and the moduli of $c_i(t)$ $(i=0,1,2,3)$. Thus, with the initial condition $c_0(0)=1$ and $c_1(0)=c_2(0)=c_3(0)=0$, we have the time evolution of the system as follows:

$$c_0(t) = \frac{-h_1^2-h_2^2+h_3^2+V_2}{2V_2}\cos(E_1 t) + \frac{h_1^2+h_2^2-h_3^2+V_2}{2V_2}\cos(E_3 t), \quad (19a)$$

$$c_1(t) = \frac{1}{2\sqrt{2}h_3V_2}[\sqrt{V_1-V_2}(h_1^2-h_2^2-h_3^2-V_2)\sin(E_1 t) - \sqrt{V_1+V_2}(h_1^2-h_2^2-h_3^2+V_2)\sin(E_3 t)] \times e^{-i(\Omega_1 t+\Phi_1-\pi/2)}, \quad (19b)$$

$$c_2(t) = \frac{h_1h_2}{V_2}[\cos(E_1 t)-\cos(E_3 t)]e^{-i[(\Omega_1+\Omega_2)t+(\Phi_1+\Phi_2)]}, \quad (19c)$$

$$c_3(t) = \frac{\sqrt{2}h_1h_2h_3}{V_2}\left[\frac{\sin(E_3 t)}{\sqrt{V_1-V_2}} - \frac{\sin(E_1 t)}{\sqrt{V_1+V_2}}\right] \times e^{-i[(\Omega_1+\Omega_2+\Omega_3)t+(\Phi_1+\Phi_2+\Phi_3)-\pi/2]}, \quad (19d)$$

where $V_1=h_1^2+h_2^2+h_3^2$ and $V_2=\sqrt{V_1^2-4h_1^2h_3^2}$. The expected maximally entangled GHZ state $|\Psi_{\mathrm{GHZ}}\rangle$ requires that the basis states $|0\rangle$ and $|3\rangle$ be simultaneously populated with equal amplitudes, i.e., $|c_0(t_0)|^2=|c_3(t_0)|^2=1/2$ and $|c_1(t_0)|^2=|c_2(t_0)|^2=0$. From Eqs. (19a)–(19d), one can deduce two sets of parameters of the magnetic pulse to generate $|\Psi_{\mathrm{GHZ}}\rangle$. The first set of pulse parameters is that $h_1=h_3$, $h_2/h_1=6/\sqrt{7}$, and the pulse duration time $t_0=\pi/(4E_3)$. Then the phase ϕ in the GHZ state $|\Psi_{\mathrm{GHZ}}\rangle=(|000\rangle+e^{i\phi}|111\rangle)/\sqrt{2}$ is determined by $\phi=\pi/2-\Sigma_{i=1}^{3}(\Omega_i t_0+\Phi_i)$, where Φ_i are the phases of the required three-frequency pulse. The second set of pulse parameters is that $h_1=h_3$, $h_2/h_1=2/\sqrt{15}$, and the pulse duration time $t_0=3\pi/(4E_3)$. The phase ϕ in the GHZ state is $\phi=-\pi/2-\Sigma_{i=1}^{3}(\Omega_i t_0+\Phi_i)$.

According to the two sets of parameters of the magnetic pulse, the generation processes of the GHZ state as a function of time are shown in Fig. 6 (for the first set of parameters) and Fig. 7 (for the second set of parameters), respectively, for the parameters $\omega_1/(2\pi)=500$ MHz, $\omega_2/(2\pi)=250$ MHz, $\omega_3/(2\pi)=100$ MHz, $J_{12}/(2\pi)=20$ MHz, $J_{23}/(2\pi)=10$ MHz, $J_{13}/(2\pi)=2$ MHz, $\Omega_1/(2\pi)=511$ MHz, $\Omega_2/(2\pi)=245$ MHz, $\Omega_3/(2\pi)=94$ MHz, and $h_1/(2\pi)=0.1$ MHz. From Figs. 6 and 7, a single-step operation is presented to produce the maximally entangled GHZ state of three qubits in the NMR model by using a three-frequency pulse with well-defined frequencies, phases, amplitudes, and duration time.

IV. GENERALIZATION TO GENERATE *N*-QUBIT ENTANGLED STATES

The single-step operation in Secs. II and III can be generalized to an *N*-qubit NMR model. The cat state for *N* qubits

is defined by $|\Psi_{\text{cat}}\rangle=(|00\cdots0\rangle+e^{i\phi}|11\cdots1\rangle)/\sqrt{2}$. Generally speaking, for an N-qubit NMR model, we use a rectangular circularly polarized transversal magnetic field pulse with N frequencies Ω_1, $\Omega_2,\ldots,$ and Ω_N. The effective Hamiltonian is

$$H_{\text{total}}^{(N)}=H_{N\ \text{qubit}}+H_{\text{pulse}}^{(N)}, \tag{20}$$

where

$$H_{N\ \text{qubit}}=-\frac{1}{2}\sum_{i=1}^{N}\left(\omega_i\sigma_i^z+\sum_{j=2(j>i)}^{N}\frac{J_{ij}}{2}\sigma_i^z\sigma_j^z\right), \tag{21}$$

$$H_{\text{pulse}}^{(N)}=-\frac{1}{4}\sum_{i,k=1}^{N}h_{ik}(e^{i(\Omega_k t+\Phi_k)}\sigma_i^{+}+e^{-i(\Omega_k t+\Phi_k)}\sigma_i^{-}). \tag{22}$$

We assume that $\omega_1>\omega_2>\cdots>\omega_N$ and $J_{ij}\ll\omega_i-\omega_j$. $H_{N\ \text{qubit}}$ has 2^N basis states and eigenenergies. $N+1$ basis states are chosen as active states. The frequency Ω_i corresponds to the resonant frequency of the transition from the ith active state to the $(i+1)$th active state and all pulse frequencies Ω_i $(i=1,2,\ldots,N)$ are required to be different. Moreover, according to the conservation laws of energy and angular momentum, all pulse frequencies Ω_i are also required not to induce a change of the remaining 2^N-N-1 inactive states. This is a necessary condition for our scheme. Thus, the system is reduced to an $(N+1)$-level subspace consisting of $N+1$ active states. For convenience, we again use decimal notation to denote the $N+1$ active states, i.e., j_{00} is denoted by j_{0i} and j_{11} by j_{Ni}, etc. Then the Hamiltonian (20) is truncated approximately as

$$H^{(N)}=\sum_{n=0}^{N}\varepsilon_n|n\rangle\langle n|+\sum_{n=1}^{N}\left(\frac{h_n}{2}e^{i(\Omega_n t+\Phi_n)}|n-1\rangle\langle n|+\text{H.c.}\right). \tag{23}$$

The evolution of the quantum state $|\Psi(t)\rangle$ under the Hamiltonian $H^{(N)}$ (23) can be expressed as

$$|\Psi(t)\rangle=\sum_{n=0}^{N}c_n(t)|n\rangle. \tag{24}$$

Likewise, the generalized rotating frame [42,44] is applied to eliminate the time dependence of $H^{(N)}$ by means of a unitary transformation

$$U(t)=\sum_{n=0}^{N}\left[\left(\prod_{m=0}^{n}e^{i(\Omega_m t+\Phi_m)}\right)|n\rangle\langle n|\right], \tag{25}$$

such that an equivalent Hamiltonian $H_{\text{rot}}^{(N)}$ is obtained,

$$H_{\text{rot}}^{(N)}=\begin{bmatrix}0 & \frac{h_1}{2} & 0 & \cdots & 0\\ \frac{h_1}{2} & 0 & \frac{h_2}{2} & \ddots & \vdots\\ 0 & \frac{h_2}{2} & 0 & \ddots & 0\\ \vdots & \ddots & \ddots & \ddots & \frac{h_N}{2}\\ 0 & \cdots & 0 & \frac{h_N}{2} & 0\end{bmatrix}. \tag{26}$$

$H_{\text{rot}}^{(N)}$ has $N+1$ eigenstates $|\eta_i\rangle=\Sigma_{n=0}^{N}v_{i(n+1)}|n\rangle$, for $i=1,2,\ldots,(N+1)$ with the eigenvalues $\eta_1,\eta_2,\ldots,\eta_{N+1}$. Propagators of the form $U^{+}(t)e^{-iH_{\text{rot}}^{(N)}t}$ determine the phases and the moduli of $c_n(t)$, from the initial state $|\Psi(0)\rangle=|00\cdots0\rangle$, and

$$c_n(t)=\left(\prod_{m=0}^{n}e^{-i(\Omega_m t+\Phi_m)}\right)\sum_{j=1}^{N+1}[(v^{-1})_{1j}e^{-i\eta_j t}v_{j(n+1)}]. \tag{27}$$

The expected cat states $|\Psi_{\text{cat}}\rangle$ require that the basis states $|00\cdots0\rangle$ (i.e., $|0\rangle$ in decimal notation) and $|11\cdots1\rangle$ (i.e., $|N\rangle$) are simultaneously populated with equal amplitudes, i.e., $|c_0(t_0)|^2=|c_N(t_0)|^2=1/2$ and the remaining $|c_n(t_0)|^2=0$. Now, our task becomes to solve N nonlinear equations to determine the pulse parameters. For larger N, it is not easy to give analytic solutions of $c_n(t)$, so numerical calculations will be invoked. According to our calculations, we find two rules (but not mathematically proved) for calculating the magnetic pulse parameters to reach the cat states for the cases of even qubits and odd qubits, respectively.

(i) For even qubits, $H_{\text{rot}}^{(N)}$ has $N+1$ eigenvalues denoted by $0,\ \pm|E_1|,\ \pm|E_2|,\ldots,\ \pm|E_{N/2}|$ with order $|E_{N/2}|>\cdots>|E_2|>|E_1|$. There are two schemes of pulse parameter sets that can reach the cat state. The first one is that $h_1=h_N,\ h_2=h_{N-1},\ldots,\ h_{(N/2)-1}=h_{(N/2)+2},\ h_{(N/2)+1}/h_{N/2}=1+\sqrt{2}$, and the duration time of the pulse $t_0=\pi/|E_1|$. In this case, the phase ϕ in the cat state $|\Psi_{\text{cat}}\rangle=(|00\cdots0\rangle+e^{i\phi}|11\cdots1\rangle)/\sqrt{2}$ is determined by $\phi=\pi-\Sigma_{m=1}^{N}(\Omega_m t_0+\Phi_m)$. The second set is $h_1=h_N,\ h_2=h_{N-1},\ldots,\ h_{(N/2)-1}=h_{(N/2)+2},\ h_{(N/2)+1}/h_{N/2}=-1+\sqrt{2}$, the duration time of the pulse $t_0=\pi/|E_1|$, and $\phi=-\Sigma_{m=1}^{N}(\Omega_m t_0+\Phi_m)$.

(ii) For odd qubits, $H_{\text{rot}}^{(N)}$ has $N+1$ eigenvalues $\pm|E_1|,\ \pm|E_2|,\ldots,\ \pm|E_{(N+1)/2}|$ with $|E_{(N+1)/2}|>\cdots>|E_2|>|E_1|$. There are again two schemes of parameter sets to reach the cat state. The first one is $h_1=h_N,\ h_2=h_{N-1},\ldots,\ h_{(N-1)/2}=h_{(N+3)/2}$, and the duration time of the pulse $t_0=\pi/(4|E_1|)$. The phase ϕ is given by $\phi=-\pi/2-\Sigma_{m=1}^{N}(\Omega_m t_0+\Phi_m)$ for $N=5,9,13,\ldots$ and $\phi=\pi/2-\Sigma_{m=1}^{N}(\Omega_m t_0+\Phi_m)$ for $N=7,11,15,\ldots$. The second set, likewise, has $h_1=h_N,\ h_2=h_{N-1},\ldots,$ and $h_{(N-1)/2}=h_{(N+3)/2}$, but $t_0=3\pi/(4|E_1|)$, and phase $\phi=-\pi/2-\Sigma_{m=1}^{N}(\Omega_m t_0+\Phi_m)$ for $N=7,11,15,\ldots$ and $\phi=\pi/2-\Sigma_{m=1}^{N}(\Omega_m t_0+\Phi_m)$ for $N=5,9,13,\ldots$.

Using these rules, numerical calculations will be simplified. We check the rules for seven cases: $N=4,5,\ldots,10$. The

TABLE I. The numerical calculation results that generate the cat states $|\Psi_{\text{cat}}\rangle$ for the N-qubit NMR model using the first scheme of parameters. $h_1/(2\pi)=0.1$ MHz and the units of t_0 are $(2\pi\ \text{MHz})^{-1}$.

N	t_0	h_2/h_1	h_3/h_1	h_4/h_1	h_5/h_1	h_6/h_1	h_7/h_1	h_8/h_1	h_9/h_1	h_{10}/h_1
4	62.83	0.6629	1.6002	1						
5	71.98	1.3801	0.6547	1.3801	1					
6	76.95	1.2910	0.7654	1.8478	1.2910	1				
7	81.62	1.2766	1.1386	2.3094	1.1386	1.2766	1			
8	88.86	1.3229	1.5000	0.8557	2.0658	1.5000	1.3229	1		
9	95.26	1.3396	1.5560	1.8150	0.8242	1.8150	1.5560	1.3396	1	
10	99.35	1.3416	1.5492	1.6733	0.9374	2.2630	1.6733	1.5492	1.3416	1

results exactly prove the rules. All numerical results are given in Tables I and II. The relation of $\ln t_0$ and $\ln N$ (for $4\leqslant N\leqslant 10$) is fitted as a curve $\ln t_0 \simeq 3.46+0.49 \ln N$, which is plotted in Fig. 8. Thus, the duration time t_0 is approximately proportional to $\sqrt{N}$. In the introduction, we mentioned that the entangled state $(|00\cdots0\rangle+|11\cdots1\rangle)/\sqrt{2}$ (the cat state) can be prepared using a Hadamard gate followed by $N-1$ controlled-NOT gates, that is, using a special sequence of magnetic pulses. As a simplified description, we assume that the operation time of a Hadamard gate is t_H and the time of each controlled-NOT gate is t_C. Then the total operation time t_0 for generating the cat state of the N-qubit NMR model by means of this special sequence of magnetic pulses is $t_0=t_H+Nt_C$, which is approximately proportional to N. According to the single-spin transition scheme for operating the controlled-NOT gate in Refs. [38–40], $t_C=\pi/\Omega$ and $t_H=\pi/(2\Omega)$ (Ω is the Rabi frequency). For comparison, we assume $\Omega/(2\pi)=0.1$ MHz. Figure 8 also shows the relation of $\ln t_0$ and $\ln N$ (indicated by black circles) needed to generate the cat states using a Hadamard gate followed by $(N-1)$ controlled-NOT gates in the N-qubit NMR model.

V. CONCLUSION

In conclusion, we described how to design a single pulse of multifrequency coherent magnetic radiation to produce maximally entangled states in the multiqubit NMR model. Unlike the previous schemes using a special sequence of magnetic pulses, our proposal is a single-step operation. In our scheme, for an N-qubit NMR system, a pulse with N nonequal frequencies is applied to manipulate simultaneously N active states. Moreover, all the pulse frequencies Ω_i are also required not to induce evolution of the remaining 2^N-N-1 inactive states. This is a necessary condition for our scheme. We obtain the magnetic pulse parameters, such as frequencies, phases, amplitudes, and duration time, necessary to implement Bell states of two qubits and GHZ states of three qubits. Generally, we find two rules for calculating the magnetic pulse parameters to reach the entangled states for even and odd qubits, respectively. We have checked the rules in several cases for $4\leqslant N\leqslant 10$ and all exactly tally with the rules. We fit the relation of $\ln t_0$ and $\ln N$, and find the duration time $t_0\sim\sqrt{N}$. In our method, a 2^N-dimensional space is reduced to an $(N+1)$-level subspace if the necessary condition is satisfied.

Theoretically, the present scheme can be extended to larger N-qubit NMR models. In practice the scheme requires the application of line selective pulses. This is easily achievable for small molecules containing several qubits, but may be difficult for larger molecules since the required J couplings become quite small for spins that are separated by several bonds. Therefore, this scheme may be practical only for a small number of qubits. On the other hand, this scheme may find useful applications in multilevel systems. For example, the Hamiltonians of Eqs. (8) and (18) can be easily implemented in multilevel systems (e.g., systems with smaller spin number S, say $S=1$ and $3/2$). Higher-order spin systems have limitations in quantum computing as well, but many other quantum computer systems rely on employing, at least temporarily, other energy levels. For example, ion trap quantum computers regularly employ other transitions to

TABLE II. The numerical calculation results that generate the cat states $|\Psi_{\text{cat}}\rangle$ for the N-qubit NMR model using the second scheme of parameters. $h_1/(2\pi)=0.1$ MHz and the units of t_0 are $(2\pi\ \text{MHz})^{-1}$.

N	t_0	h_2/h_1	h_3/h_1	h_4/h_1	h_5/h_1	h_6/h_1	h_7/h_1	h_8/h_1	h_9/h_1	h_{10}/h_1
4	62.83	1.6002	0.6629	1						
5	67.26	1.0091	2.1020	1.0091	1					
6	76.95	1.2910	1.8478	0.7654	1.2910	1				
7	84.00	1.3275	1.6194	0.7480	1.6194	1.3275	1			
8	88.86	1.3229	1.5000	2.0658	0.8557	1.5000	1.3229	1		
9	93.31	1.3225	1.4772	1.2598	2.5252	1.2598	1.4772	1.3225	1	
10	99.35	1.3416	1.5492	1.6733	2.2630	0.9374	1.6733	1.5492	1.3416	1

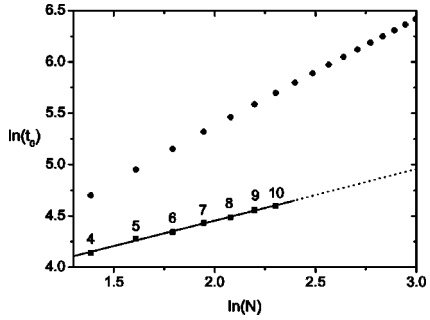

FIG. 8. The relation of ln t_0 and ln N. The black squares indicate the numerical calculation results for the N-qubit NMR model using a single-step operation to generate the cat states. The numbers above the black squares present the number of qubits in the NMR model. The solid line is the linearly fitted one, and the dotted line is an extrapolated one. The black circles indicate the relation of ln t_0 and ln N for generating the cat states using a Hadamard gate followed by $N-1$ controlled-NOT gates in the N-qubit NMR model.

temporarily move the quantum state out of the qubit manifold. In another example using coupled Josephson junctions, higher-lying energy levels could be used to implement two-qubit gates. Our scheme may find the most applications in such schemes, which lie outside spin-1/2 NMR quantum computing. Meanwhile, it should be noted that off-resonance pulses induce z rotations even far beyond the excitation window of the pulse [46]. These z rotations are the results of transient Bloch-Siegert shifts [46–48]. The shifts have unfavorable effects on this proposed scheme, especially for the case of nearby frequencies, because the quantum state during the pulse itself is rather complicated and most definitely not a computational basis state. Fortunately, Steffen *et al*. found that the resulting error from transient Bloch-Siegert shifts can be corrected by shifting the frequency of the on-resonance pulse in such a way that it tracks the shift of the spin frequency [49]. Briefly, although in practice this proposed scheme is subject to the choice of the system, its advantage may be to provide a possible scheme for designing the shortest sequence of pulses corresponding to a quantum computation task.

ACKNOWLEDGMENTS

B.Z. acknowledges the support from the China Postdoctoral Science Foundation (Grant No. 2002032138) and the National Natural Science Foundation of China (Grant No. 10347106). R.B.T. acknowledges support from the National Natural Science Foundation of China (Grants No. 10174015 and No. 10234010) and the 973 Project of China (Grant No. 2002CB613504). S.Q.S. acknowledges support from the Research Grants Council of Hong Kong (Grant No. HKU7023/03P).

APPENDIX

Four eigenstates (not normalized) of $H_{\mathrm{rot}}^{(3)}$ are

$$|\varphi_1\rangle = \frac{\sqrt{V_1+V_2}(-h_1^2-h_2^2+h_3^2+V_2)}{2\sqrt{2}h_1h_2h_3}|0\rangle + \frac{-h_1^2+h_2^2+h_3^2+V_2}{2h_1h_2}|1\rangle + \frac{\sqrt{V_1+V_2}}{\sqrt{2}h_1}|2\rangle + |3\rangle,$$

$$|\varphi_2\rangle = \frac{\sqrt{V_1+V_2}(h_1^2+h_2^2-h_3^2-V_2)}{2\sqrt{2}h_1h_2h_3}|0\rangle + \frac{-h_1^2+h_2^2+h_3^2+V_2}{2h_1h_2}|1\rangle - \frac{\sqrt{V_1+V_2}}{\sqrt{2}h_1}|2\rangle + |3\rangle,$$

$$|\varphi_3\rangle = \frac{-\sqrt{V_1-V_2}(h_1^2+h_2^2-h_3^2+V_2)}{2\sqrt{2}h_1h_2h_3}|0\rangle + \frac{-h_1^2+h_2^2+h_3^2-V_2}{2h_1h_2}|1\rangle + \frac{\sqrt{V_1-V_2}}{\sqrt{2}h_1}|2\rangle + |3\rangle,$$

$$|\varphi_4\rangle = \frac{\sqrt{V_1-V_2}(h_1^2+h_2^2-h_3^2+V_2)}{2\sqrt{2}h_1h_2h_3}|0\rangle + \frac{-h_1^2+h_2^2+h_3^2-V_2}{2h_1h_2}|1\rangle - \frac{\sqrt{V_1-V_2}}{\sqrt{2}h_1}|2\rangle + |3\rangle,$$

where $V_1=h_1^2+h_2^2+h_3^2$ and $V_2=\sqrt{V_1^2-4h_1^2h_3^2}$. The eigenvalues are given by $E_1=\sqrt{V_1+V_2}/(2\sqrt{2})$, $E_2=-\sqrt{V_1+V_2}/(2\sqrt{2})$, $E_3=\sqrt{V_1-V_2}/(2\sqrt{2})$, and $E_4=-\sqrt{V_1-V_2}/(2\sqrt{2})$.

[1] S. Lloyd, Science **261**, 1569 (1993).
[2] D. P. DiVincenzo, Science **269**, 255 (1995).
[3] J. I. Cirac and P. Zoller, Phys. Rev. Lett. **74**, 4091 (1995); C. Monroe, D. M. Meekhof, B. E. King, W. M. Itano, and D. J. Wineland, *ibid.* **75**, 4714 (1995).
[4] N. A. Gershenfeld and I. L. Chuang, Science **275**, 350 (1997); D. Cory, A. Fahmy, and T. Havel, Proc. Natl. Acad. Sci. U.S.A. **94**, 1634 (1997).
[5] Q. A. Turchette, C. J. Hood, W. Lange, H. Mabuchi, and H. J. Kimble, Phys. Rev. Lett. **75**, 4710 (1995).
[6] A. Shnirman, G. Schön, and Z. Hermon, Phys. Rev. Lett. **79**, 2371 (1997).
[7] D. Loss and D. P. DiVincenzo, Phys. Rev. A **57**, 120 (1998).
[8] B. E. Kane, Nature (London) **393**, 133 (1998).
[9] I. L. Chuang, L. M.K. Vandersypen, X. L. Zhou, D. W. Leung, and S. Lloyd, Nature (London) **393**, 143 (1998).
[10] K. Dorai, Arvind, and A. Kumar, Phys. Rev. A **61**, 042306 (2000).
[11] R. Marx, A. F. Fahmy, J. M. Myers, W. Bermel, and S. J. Glaser, Phys. Rev. A **62**, 012310 (2000).

[12] J. A. Jones, M. Mosca, and R. H. Hansen, Nature (London) **393**, 344 (1998).
[13] I. L. Chuang, N. Gershenfeld, and M. Kubinec, Phys. Rev. Lett. **80**, 3408 (1998).
[14] L. M.K. Vandersypen, M. Steffen, M. H. Sherwood, C. S. Yannoni, G. Breyta, and I. L. Chuang, Appl. Phys. Lett. **76**, 646 (2000).
[15] L. M.K. Vandersypen, M. Steffen, G. Breyta, C. S. Yannoni, M. H. Sherwood, and I. L. Chuang, Nature (London) **414**, 883 (2001).
[16] D. G. Cory, M. D. Price, W. Maas, E. Knill, R. Laflamme, W. H. Zurek, T. F. Havel, and S. S. Somaroo, Phys. Rev. Lett. **81**, 2152 (1998).
[17] E. Knill, R. Laflamme, R. Martinez, and C. Negrevergne, Phys. Rev. Lett. **86**, 5811 (2001).
[18] Y. S. Weinstein, M. A. Pravia, E. M. Fortunato, S. Lloyd, and D. G. Cory, Phys. Rev. Lett. **86**, 1889 (2001).
[19] L. M.K. Vandersypen, M. Steffen, G. Breyta, C. S. Yannoni, R. Cleve, and I. L. Chuang, Phys. Rev. Lett. **85**, 5452 (2000).
[20] M. A. Nielsen, E. Knill, and R. Laflamme, Nature (London) **396**, 52 (1998).
[21] M. Steffen, W. van Dam, T. Hogg, G. Breyta, and I. Chuang, Phys. Rev. Lett. **90**, 067903 (2003).
[22] L. Viola, E. M Fortunato, M. A. Pravia, E. Knill, R. Laflamme, and D. G. Cory, Science **293**, 2059 (2001).
[23] J. E. Ollerenshaw, D. A. Lidar, and L. E. Kay, Phys. Rev. Lett. **91**, 217904 (2003).
[24] J. A. Jones, V. Vedral, A. Ekert, and G. Castagnoli, Nature (London) **403**, 869 (2000).
[25] J. Du, P. Zou, M. Shi, L. C. Kwek, J.-W. Pan, C. H. Oh, A. Ekert, D. K.L. Oi, and M. Ericsson, Phys. Rev. Lett. **91**, 100403 (2003).
[26] J. S. Bell, Physics (Long Island City, N.Y.) **1**, 195 (1965).
[27] D. M. Greenberger, M. A. Horne, and A. Zeilinger, Am. J. Phys. **58**, 1131 (1990).
[28] C. H. Bennett, Phys. Scr., T **76**, 210 (1998).
[29] A. Galindo and M. A. Martin-Delgado, Rev. Mod. Phys. **74**, 347 (2002).
[30] I. L. Chuang, N. Gershenfeld, M. G. Kubinec, and D. W. Leung, Proc. R. Soc. London, Ser. A **454**, 447 (1998).
[31] S. Lloyd, Phys. Rev. A **57**, R1473 (1998).
[32] R. Laflamme, E. Knill, W. H. Zurek, P. Catasti, and S. V.S. Mariappan, Philos. Trans. R. Soc. London, Ser. A **356**, 1941 (1998).
[33] R. J. Nelson, D. G. Cory, and S. Lloyd, Phys. Rev. A **61**, 022106 (2000).
[34] E. Knill, R. Laflamme, R. Martinez, and C. H. Tseng, Nature (London) **404**, 368 (2000).
[35] N. Boulant, E. M. Fortunato, M. A. Pravia, G. Teklemariam, D. G. Cory, and T. F. Havel, Phys. Rev. A **65**, 024302 (2002).
[36] S. Lloyd, Sci. Am. **273**, 140 (1995).
[37] J. A. Jones, Prog. Nucl. Magn. Reson. Spectrosc. **38**, 325 (2001).
[38] J. Du, M. Shi, J. Wu, X. Zhou, and R. Han, Phys. Rev. A **63**, 042302 (2001).
[39] G. P. Berman, D. K. Campbell, G. D. Doolen, G. V. López, and V. I. Tsifrinovich, Physica B **240**, 61 (1997).
[40] G. P. Berman, G. D. Doolen, G. V. López, and V. I. Tsifrinovich, Phys. Rev. B **58**, 11 570 (1998).
[41] M. N. Leuenberger and D. Loss, Nature (London) **410**, 789 (2001).
[42] M. N. Leuenberger, D. Loss, M. Poggio, and D. D. Awschalom, Phys. Rev. Lett. **89**, 207601 (2002).
[43] B. Zhou, R. Tao, S.-Q. Shen, and J.-Q. Liang, Phys. Rev. A **66**, 010301 (2002).
[44] A. Abragam, *The Principles of Nuclear Magnetism* (Clarendon, Oxford, 1961).
[45] A trivial term $(\varepsilon_1+\Omega_1)I$ has been ignored in the Hamiltonian (I is a 3×3 unit matrix), which does not affect the final results we discuss.
[46] L. Emsley and G. Bodenhausen, Chem. Phys. Lett. **168**, 297 (1990).
[47] F. Bloch and A. Siegert, Phys. Rev. **57**, 522 (1940).
[48] N. F. Ramsey, Phys. Rev. **100**, 1191 (1955).
[49] M. Steffen, L. M.K. Vandersypen, and I. L. Chuang, J. Magn. Reson. **146**, 369 (2000).